Energy Proceedings
Vol 31, 2023
ISSN 2004-2965

Research on the Application of Cooling Modules with Inorganic Phase Change Materials in the Thermal Management of Lithium-ion Batteries

Hanxue Yang[1], Guanhua Zhang[1*], Xiaoyu Yan[2]
[1]School of Energy and Power Engineering, University of Shanghai for Science and Technology, Shanghai, 200093, China
[2]Environment and Sustainability Institute, University of Exeter, Penryn, Cornwall, TR10 9FE, UK
[*]Corresponding author. E-mail address: guanhuazhang@usst.edu.cn

ABSTRACT

Lithium-ion batteries generate a lot of heat during discharge, which can cause the risk of excessive temperature and accelerate the capacity fading rate. Cooling the battery through the latent heat storage of hydrated salt is a good choice. In this study, hydrated salts mixed with sodium acetate trihydrate and disodium hydrogen phosphate dodecahydrate were modified to change the phase change temperature and enthalpy, and then the battery cooling modules were prepared by using modified composite phase change material as a filler and copper foam as a support matrix. The thermal performance of the modified composite phase change material was tested and analyzed by differential scanning calorimetry (DSC) test. The DSC analysis showed that the composite phase change material with 5wt% sodium acetate trihydrate had the best performance, the enthalpy was 278.9 kJ/kg and its phase change temperature was 46.9 ℃. The results of the surface temperature measurement experiments of the cooling module on the battery showed that the cooling module can effectively reduce the temperature in the discharge process and the maximum temperature reduction can be up to 9 ℃. The lowest temperature was 55 ℃ with the battery cooling module on the discharge at 1.5C.

Keywords: hydrated salts, phase change material, battery cooling modules, Lithium-ion battery

1. INTRODUCTION

Nearly 30% of global greenhouse gas emissions come from conventionally-fueled road transport and contribute to air quality and environmental problems worldwide [1]. The focus of research has therefore turned to clean energy vehicles, which operate without harmful substances being released directly into the environment. The energy storage in electric vehicles is electrochemical batteries, with lithium-ion batteries being the most used today. Lithium-ion batteries are promising candidates for their high energy density, low self-discharge rate, long cycle life and high discharge voltage [2-4]. During vehicle use, the battery discharges and generates considerable heat due to the electrochemical reactions in the battery. Therefore, the heat generated by the battery needs to be discharged to maintain the safe operating temperature allowed for the battery [5, 6]. Early studies have shown that if the temperature of a Li-ion battery exceeds 50 ℃, the life cycle and rechargeability of the battery is significantly reduced [7]. Safe operating temperatures are typically reported to be within the range of 20-40 ℃ [8]. Higher temperatures in a battery can reduce its cycling performance and lead to thermal runaway and eventually battery explosion. The maximum temperature difference range should be limited to 5 °C when the battery is in operation [9]. The battery pack may face several problems, such as overcharging, over discharging or short-circuiting due to uneven charging or discharging of the battery. In addition, temperature inhomogeneity increases with increasing discharge rate [10].

The thermal problems associated with safe battery operating conditions described above have been addressed by the use of a Battery Thermal Management System (BTMS). In most cases, the design of the BTMS varies depending on the workpiece used to dissipate the heat from the battery. Many studies have reported on

battery cooling with air and liquid as the cooling media [11-13]. Some of the issues associated with air/liquid cooled BTMS are the need for air/liquid distribution systems, pumping accessories and power consumption [14]. The application of phase change materials in BTMS reduces the complexity of the system components. Al-Hallaj and Selman [15] first introduced the concept of phase change regulation in cell cooling and showed a reduction in cell temperature and a better uniformity of temperature in the cell. They also studied cylindrical cells analytically and estimated the reduction in cell temperature in the cooling system employed by PCM. Analysis of the ageing behavior of PCM-cooled prismatic cells has been reported by Rao et al. [16]. khateeb et al. [17] presented simulation results for a Li-ion battery module operating at a higher ambient temperature of 40°C. At an initial temperature of about 25°C, the temperature rise was up to 40°C, similar to the wide range of ambient temperatures from 20°C to 55°C proposed by Fathabadi [18], where a comparison of combined PCM cooling in free convection and forced convection modes shows that such a system can limit the temperature to below 60°C.

Some researchers have also used multiple layers of phase change materials to cool the batteries [19, 20]. Although it has been effective in cooling down the batteries, it is mainly organic phase change materials that are used. Organic phase change materials also suffer from leakage problems and most applications require additional wrapping material on the outside, thus drastically reducing the thermal conductivity. Organic phase change materials have the disadvantage of being flammable and can easily cause fires when thermal runaway occurs in the battery. The use of inorganic phase change materials has therefore become a new research direction [21, 22]. The main inorganic phase change materials are hydrated salts, whose heat of phase change depends on the strength of bonding between separated water molecules [23]. The phase change temperature of hydrated salts can range from a few degrees Celsius to over 100 °C. The main hydrated salt phase change materials include magnesium chloride hexahydrate [24], sodium sulphate decahydrate [25, 26], sodium carbonate heptahydrate [27] and sodium acetate trihydrate [28]. However, most phase change materials inevitably suffer from phase changes, supercooling and lower thermal conductivity during phase change. Different additives and controlled mass fractions are added to improve the properties [29].

Sodium acetate trihydrate (SAT) has received increasing attention among phase change energy storage materials [30-32] due to its suitable phase change temperature (58.4°C) and high latent heat of phase change (264 kJ/kg). It is also characterized by a low coefficient of phase change expansion, good chemical stability, non-toxicity and low cost. Not surprisingly, as a hydrated salt phase change material, SAT suffers from high subcooling, phase delamination, low thermal conductivity (0.4~0.7W/(m·K)) [33-35] and corrosion with commonly used metals (copper, aluminium, stainless steel) [36]. A great deal of work has been done in the preparation of composite phase change materials. Different nucleating agents, thickeners and phase change thermoregulators have been experimentally selected for application to SAT matrices to overcome these problems to some extent [37-39].

Based on this research background, this paper attempts to prepare composite phase change materials (CPCM). The thermal properties of the new composites were investigated by experimentally applying disodium hydrogen phosphate dodecahydrate (DHPD) to the SAT combines. The composite phase change materials were added to copper foam and the whole was used as a battery cooling module (BCM) in temperature control experiments for battery discharge in order to determine their applicability in BTMS. The present study provides practical guidance for the design and optimization of thermal management structure for Lithium-ion batteries.

2. EXPERIMENTAL

2.1 Materials

In the experiments, SAT, DHPD, aluminum oxide nanoparticles and carboxymethyl cellulose (CMC) supplied by Shanghai Maclean Company were selected for blending. The copper foam used in this experiment was supplied by Suzhou Jiaside Metal Foam Co. We chose a copper foam with a porosity of 85% and a pore density of 50 ppi. The square battery used in this experiment was purchased from Tianjin Shenli Co., the exact dimensions of which are indicated in Fig. 2. The batteries are rated at 4.4V and have a total capacity of 4590mAh.

2.2 Preparation method

All substances were accurately weighed and mixed. For experimental accuracy, the mass of each sample was set at 20 g. The proportions of the components in the samples are shown in Table 1 and the required mass of each substance was weighed on an electronic balance. SAT was first added and stirred and heated for 10 minutes, then DHPD was added, mixed and heated again

for 10 minutes and finally alumina nanoparticles and CMC were added, each sample was heated uniformly in an oil bath maintained at 110 ℃. The stirrer was kept in the flask at 1100 r/min to ensure the samples were well mixed and the beaker was sealed during this process. Finally, the samples were cooled and solidified at room temperature.

In order to cool down the battery, the copper foam is cut into squares of 25 mm on each side and the thickness of the copper foam is uniformly 5 mm. The melt impregnation method was used to prepare a battery cooling module (BCM) containing a composite phase change material. The preparation process is illustrated in Fig. 1.

Table 1 Components of composite phase change materials

Component / Sample	SAT (w%)	DHPD (w%)	CMC (w%)	Nano Al_2O_3 (w%)
S1	0.00	91.50	3.50	5.00
S2	5.00	86.50	3.50	5.00
S3	45.75	45.75	3.50	5.00
S4	51.50	40.00	3.50	5.00
S5	71.50	20.00	3.50	5.00
S6	81.50	10.00	3.50	5.00
S7	84.00	7.50	3.50	5.00
S8	86.50	5.00	3.50	5.00
S9	91.50	0.00	3.50	5.00

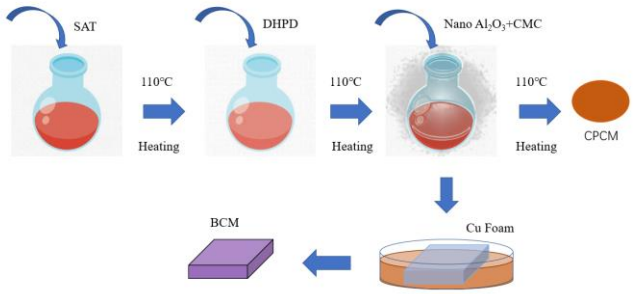

Fig. 1. Process for the preparation of CPCMs and BCMs

2.3 *Characterizations*

The phase change behavior of the worthy composite phase change material was characterized using a differential scanning calorimeter (Netzsch DSC-200PCPhox, Germany) at a heating level of 2 °C/min. All tests are carried out at room temperature and in a nitrogen-protected environment.

The temperature of the surface of the cell was measured by means of a T-type thermocouple, as shown in Fig. 2. Five measurement points (a, b, c, d, e) were set up on the cell, at the two pole lugs and at each quarter of the cell. The temperature of the discharged surface of the cell at different multiplier conditions was measured both before and after the placement of the phase change cooling module. The entire experiment was carried out at an ambient temperature of 25 ℃.

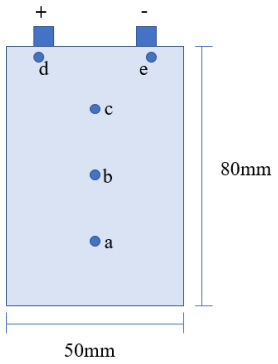

Fig. 2. Battery parameters and thermocouple position

3. RESULTS AND DISCUSSION

3.1 *Thermal properties*

Nine sets of samples from S1 to S9 were obtained by adjusting the ratio of SAT and DHPD components in the composite phase change material. The enthalpies of these nine samples were examined and the phase change parameters obtained are listed in Table 2. The measured DSC results are shown in Fig. 3.

It is clear from Fig. 3 that there are two distinct peaks at low levels of SAT, indicating that two substances are present separately and that there are substances undergoing phase change processes at different temperatures. When the mass fraction of SAT reaches 71.5%, there is only one melting peak left on the curve, which can prove that the phase change behavior of SAT has completely influenced the change process of DHPD.

Of the nine samples, S1 and S9 did not have the largest enthalpies, but S2 had the largest enthalpy of 278.9 kJ/kg and the phase change onset temperature of the S2 sample was 46.9 °C. After S2, the enthalpy of the composite phase change materials generally tended to increase, but S7 showed a sudden drop, indicating that although the effect of DHPD on the melting peak was negligible at this point, the enthalpy of the composite phase change materials was not as high as the enthalpy of S2. The effect on the enthalpy is much greater.

As the phase change temperature point of sample S2 is near the battery alert temperature of 45 ℃ and the enthalpy of the composite phase change material is also

at its maximum at this time, the composite phase change material required for the copper foam based BCM was chosen to be prepared in the proportions corresponding to S2.

Table 2 Phase change parameters of CPCM

Sample	Onset temperature T_{mo}(℃)	End temperature T_{me}(℃)	Phase change enthalpy (kJ/kg)
S1	50.3	57.3	159.6
S2	46.9	52.5	278.9
S3	46.5	54.6	164.9
S4	44.4	52.3	179.1
S5	57.4	65.1	212.1
S6	55.8	70.5	219.0
S7	59.3	67.1	192.5
S8	57.6	67.3	230.2
S9	56.0	68.8	235.4

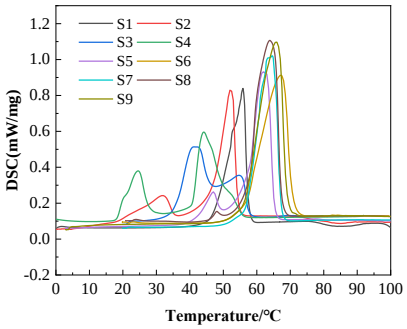

Fig. 3. Enthalpy result curves for samples S1 to S9.

3.2 Battery thermal management behavi*rs*

Due to the need for stable battery operation, there is a risk that the battery will stop working and explode if the temperature exceeds 45 ℃ during battery discharge. As shown in Fig. 4, the surface temperature variation of a battery discharged at different multipliers without the addition of the BCM is shown. It can be seen that as the magnification increases, the surface temperature of the battery also increases.

As can be seen in Fig. 4(a), the maximum temperature on the surface of the battery already reaches 45 ℃ at 0.7 C. In picture b, where the battery is discharged at 1.0 C magnification, the surface temperature of the battery rises to 57 ℃ and exceeds 45 ℃ before the battery has been discharged for more than the usual length of time. In figure c, at the end of the discharge process, the battery temperature reaches 65 ℃ and in figure d, the maximum temperature reaches 70 ℃.

A comparison of the four Fig. 4(a) to (d) graphs shows that the difference in temperature between the battery surfaces is not large, with a maximum temperature difference of 4 ℃, and that the temperature difference gradually increases as the discharge multiplier increases. What can be noticed is that the greatest increase in battery surface temperature is seen from 0.7 C to 1.0 C, with the cell surface temperature increasing from 45 ℃ to 57 ℃, an increase of 12 ℃, while from 1.0 C to 1.3 C the temperature increases by 8 ℃ and from 1.3 C to 1.5 C the temperature increases by just 5 ℃.

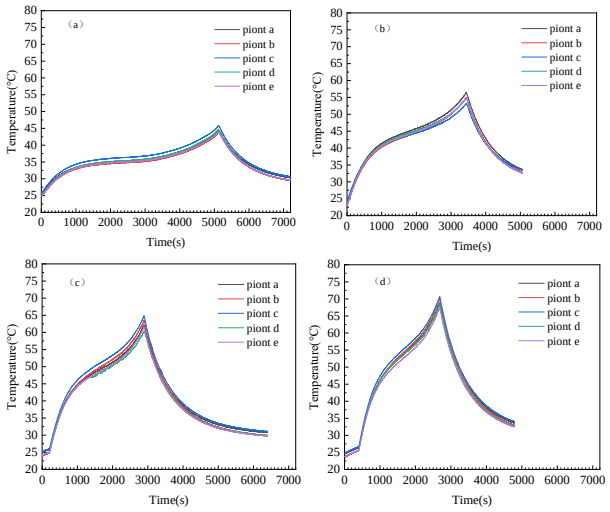

Fig. 4. Surface temperature curves of the battery without BCM at 0.7C (a), 1.0C (b), 1.3C (c) and 1.5C (d).

During the discharge of the battery a huge amount of heat is generated, causing the surface temperature of the battery to rise rapidly in a short period of time [40]. A cooling module is therefore placed on the surface of the battery in the hope that it will help to alleviate the rapidly rising surface temperature.

The maximum surface temperature of the battery at the end of the discharge in Fig. 5(a) did not exceed 45 ℃, and the maximum temperature in Fig. 5(b) is 48 ℃, the battery is basically discharged within the safe temperature. The maximum surface temperature of the battery is reduced by 9 ℃. The maximum temperature at the end of discharge in Fig. 5(c) is 58 ℃, which is a reduction of 7 ℃ compared to the case without the cooling module. Fig. 5(d) shows that the maximum temperature was 65°C and the temperature was reduced by 5°C compared to the case without the presence of the BCM.

As can be seen from figure a, the BCM is not effective in cooling the highest temperature point of the battery at 0.7 C, but the temperature in all other shops is

reduced to around 35 ℃, keeping the battery at an optimum temperature of 35 ℃ throughout the discharge process [41]. The minimum temperature on the surface of the battery at the end of discharge in Fig. 4(b) is 40 ℃, the minimum temperature on the surface at the end of discharge in Fig. 4(c) is 50 ℃ and the minimum temperature on the surface at the end of the discharge process in Fig. 4(d) is 55 ℃.

By comparing the minimum temperature at the surface of the battery with and without the BCM, it can be seen that the BCM reduces the surface temperature of the battery to a large extent at each discharge multiplier, quickly absorbing the heat generated during the discharge of the battery. With the BCM survived, the battery is able to operate safely at discharge multipliers less than 1.0 C, and at multipliers greater than 1.0 C it can significantly reduce the surface temperature of the battery.

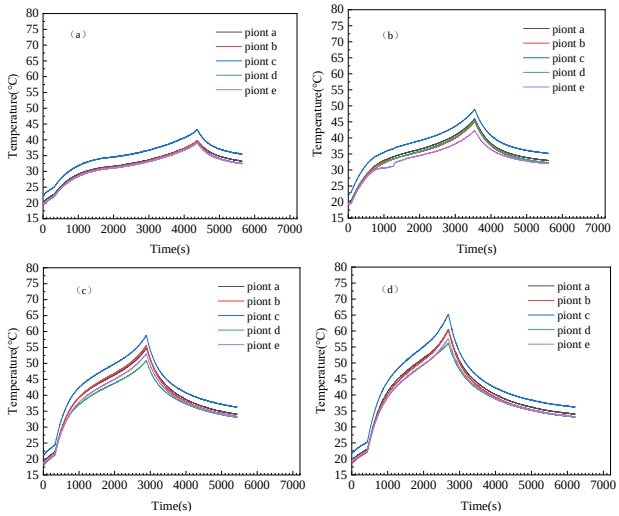

Fig. 5. Surface temperature curves of the battery with BCM at 0.7C (a), 1.0C (b), 1.3C (c) and 1.5C (d).

4. CONCLUSION

In this paper, a variety of inorganic phase change material composites with copper foam as the substrate, were used to investigate the cooling of the battery cooling. The main conclusions are summarized below.

(1) At a SAT mass fraction of 5%, the CPCM can achieve a maximum phase change enthalpy of 278.9 kJ/kg and a phase change temperature of 46.9 ℃.

(2) Without the presence of the BCM, the maximum temperature of the battery discharged at 1.0 C is 57 ℃, which is above the warning temperature, and the maximum surface temperature of the discharged at 1.5 C can reach 70 ℃.

(3) With the addition of the BCM, the surface temperature of the battery at the end of discharge is significantly reduced. The maximum surface temperature is reduced by up to 9 ℃ with a maximum temperature of 65 ℃.

ACKNOWLEDGEMENT

This work was supported by the National Natural Science Foundation of China (No.51976126), Shanghai Municipal Natural Science Foundation (No.22ZR1442700).

REFERENCE

[1] Ahmadi P. Environmental impacts and behavioral drivers of deep decarbonization for transportation through electric vehicles. Journal of cleaner production. 2019;225:1209-19.

[2] Mehrabi-Kermani M, Houshfar E, Ashjaee M. A novel hybrid thermal management for Li-ion batteries using phase change materials embedded in copper foams combined with forced-air convection. International Journal of Thermal Sciences. 2019;141:47-61.

[3] Hussain A, Abidi IH, Tso CY, Chan KC, Luo Z, Chao CY. Thermal management of lithium ion batteries using graphene coated nickel foam saturated with phase change materials. International journal of thermal sciences. 2018;124:23-35.

[4] Mallow A, Abdelaziz O, Graham S. Thermal charging performance of enhanced phase change material composites for thermal battery design. International Journal of Thermal Sciences. 2018;127:19-28.

[5] Panchal S, Dincer I, Agelin-Chaab M, Fraser R, Fowler M. Experimental investigation and simulation of temperature distributions in a 16Ah-LiMnNiCoO2 battery during rapid discharge rates. Heat and Mass Transfer. 2017;53:937-46.

[6] Panchal S, Akhoundzadeh MH, Raahemifar K, Fowler M, Fraser R. Heat and mass transfer modeling and investigation of multiple LiFePO4/graphite batteries in a pack at low C-rates with water-cooling. International Journal of Heat and Mass Transfer. 2019;135:368-77.

[7] Sato N. Thermal behavior analysis of lithium-ion batteries for electric and hybrid vehicles. Journal of power sources. 2001;99:70-7.

[8] Wang C, Lin T, Huang J, Rao Z. Temperature response of a high power lithium-ion battery subjected to high current discharge. Materials Research Innovations. 2015;19:S2-156-S2-60.

[9] Mahamud R, Park C. Reciprocating air flow for Li-ion battery thermal management to improve temperature uniformity. Journal of Power Sources. 2011;196:5685-96.

[10] Panchal S, Dincer I, Agelin-Chaab M, Fraser R, Fowler M. Transient electrochemical heat transfer modeling and experimental validation of a large sized LiFePO4/graphite battery. International Journal of Heat and Mass Transfer. 2017;109:1239-51.

[11] Jilte R, Kumar R. Numerical investigation on cooling performance of Li-ion battery thermal management system at high galvanostatic discharge. Engineering science and technology, an international journal. 2018;21:957-69.

[12] Jilte RD, Kumar R, Ma L. Thermal performance of a novel confined flow Li-ion battery module. Applied Thermal Engineering. 2019;146:1-11.

[13] Panchal S, Gudlanarva K, Tran M-K, Fraser R, Fowler M. High reynold's number turbulent model for micro-channel cold plate using reverse engineering approach for water-cooled battery in electric vehicles. Energies. 2020;13:1638.

[14] Jilte R, Kumar R, Ahmadi MH. Cooling performance of nanofluid submerged vs. nanofluid circulated battery thermal management systems. Journal of Cleaner Production. 2019;240:118131.
[15] Al-Hallaj S, Selman JR. Thermal modeling of secondary lithium batteries for electric vehicle/hybrid electric vehicle applications. Journal of power sources. 2002;110:341-8.
[16] Rao Z, Wang S, Zhang G. Simulation and experiment of thermal energy management with phase change material for ageing LiFePO4 power battery. Energy Conversion and Management. 2011;52:3408-14.
[17] Khateeb SA, Farid MM, Selman JR, Al-Hallaj S. Design and simulation of a lithium-ion battery with a phase change material thermal management system for an electric scooter. Journal of Power Sources. 2004;128:292-307.
[18] Fathabadi H. High thermal performance lithium-ion battery pack including hybrid active–passive thermal management system for using in hybrid/electric vehicles. Energy. 2014;70:529-38.
[19] Moraga NO, Xamán JP, Araya RH. Cooling Li-ion batteries of racing solar car by using multiple phase change materials. Applied Thermal Engineering. 2016;108:1041-54.
[20] Nasehi R, Alamatsaz A, Salimpour MR. Using multi-shell phase change materials layers for cooling a lithium-ion battery. Thermal Science. 2016;20:391-403.
[21] Karthick A, Murugavel KK, Ramanan P. Performance enhancement of a building-integrated photovoltaic module using phase change material. Energy. 2018;142:803-12.
[22] Li G, Hwang Y, Radermacher R, Chun H-H. Review of cold storage materials for subzero applications. Energy. 2013;51:1-17.
[23] Mohamed SA, Al-Sulaiman FA, Ibrahim NI, Zahir MH, Al-Ahmed A, Saidur R, et al. A review on current status and challenges of inorganic phase change materials for thermal energy storage systems. Renewable and Sustainable Energy Reviews. 2017;70:1072-89.
[24] Zhou S, Zhou Y, Ling Z, Zhang Z, Fang X. Modification of expanded graphite and its adsorption for hydrated salt to prepare composite PCMs. Applied Thermal Engineering. 2018;133:446-51.
[25] Ndukwu M, Bennamoun L, Abam F, Eke A, Ukoha D. Energy and exergy analysis of a solar dryer integrated with sodium sulfate decahydrate and sodium chloride as thermal storage medium. Renewable Energy. 2017;113:1182-92.
[26] Li F-y, Wang P, Yuan Y-d, Yang Y, Qian L. The preparation of phase change material Na2SO4· 10H2O with the phase transition temperature at room temperature. Synth Mater Aging Appl. 2015;44:39-46.
[27] Wang Y, Yu K, Peng H, Ling X. Preparation and thermal properties of sodium acetate trihydrate as a novel phase change material for energy storage. Energy. 2019;167:269-74.
[28] Li X, Zhou Y, Nian H, Zhu F, Ren X, Dong O, et al. Preparation and thermal energy storage studies of CH3COONa· 3H2O–KCl composites salt system with enhanced phase change performance. Applied Thermal Engineering. 2016;102:708-15.
[29] Mao J, Dong X, Hou P, Lian H. Preparation research of novel composite phase change materials based on sodium acetate trihydrate. Applied Thermal Engineering. 2017;118:817-25.
[30] Shin HK, Park M, Kim H-Y, Park S-J. Thermal property and latent heat energy storage behavior of sodium acetate trihydrate composites containing expanded graphite and carboxymethyl cellulose for phase change materials. Applied Thermal Engineering. 2015;75:978-83.
[31] Gunasekara SN, Martin V, Chiu JN. Phase equilibrium in the design of phase change materials for thermal energy storage: State-of-the-art. Renewable and Sustainable Energy Reviews. 2017;73:558-81.
[32] Xie N, Huang Z, Luo Z, Gao X, Fang Y, Zhang Z. Inorganic salt hydrate for thermal energy storage. Applied Sciences. 2017;7:1317.
[33] Fashandi M, Leung SN. Sodium acetate trihydrate-chitin nanowhisker nanocomposites with enhanced phase change performance for thermal energy storage. Solar Energy Materials and Solar Cells. 2018;178:259-65.
[34] Ma Z, Bao H, Roskilly AP. Study on solidification process of sodium acetate trihydrate for seasonal solar thermal energy storage. Solar Energy Materials and Solar Cells. 2017;172:99-107.
[35] Dannemand M, Delgado M, Lazaro A, Penalosa C, Gundlach C, Trinderup C, et al. Porosity and density measurements of sodium acetate trihydrate for thermal energy storage. Applied thermal engineering. 2018;131:707-14.
[36] Zhou G, Xiang Y. Experimental investigations on stable supercooling performance of sodium acetate trihydrate PCM for thermal storage. Solar energy. 2017;155:1261-72.
[37] Cui W, Yuan Y, Sun L, Cao X, Yang X. Experimental studies on the supercooling and melting/freezing characteristics of nano-copper/sodium acetate trihydrate composite phase change materials. Renewable Energy. 2016;99:1029-37.
[38] Mao J, Hou P, Liu R, Chen F, Dong X. Preparation and thermal properties of SAT-CMC-DSP/EG composite as phase change material. Applied Thermal Engineering. 2017;119:585-92.
[39] Kong W, Dannemand M, Johansen JB, Fan J, Dragsted J, Englmair G, et al. Experimental investigations on heat content of supercooled sodium acetate trihydrate by a simple heat loss method. Solar energy. 2016;139:249-57.
[40] Zhang Y, Hao N, Lin X, Nie S. Emerging challenges in the thermal management of cellulose nanofibril-based supercapacitors, lithium-ion batteries and solar cells: A review. Carbohydrate Polymers. 2020;234:115888.
[41] Kim J, Oh J, Lee H. Review on battery thermal management system for electric vehicles. Applied thermal engineering. 2019;149:192-212.